Operation of a SHARON nitritation reactor: practical implications from a theoretical study

E.I.P. Volcke*, M. Loccufier**, E.J.L. Noldus** and P.A. Vanrolleghem*,***

*BIOMATH, Department of Applied Mathematics, Biometrics and Process Control, Ghent University, Coupure links 653, B-9000 Gent, Belgium (E-mail: *eveline.volcke@ugent.be*)

**Department of Electrical Energy, Systems and Automation, Ghent University, Technologiepark 913, B-9052 Zwijnaarde, Belgium (E-mail: *mia.loccufier@ugent.be*; *noldus@autoctrl.ugent.be*)

***modelEAU, Département de génie civil, Pavillon Pouliot, Université Laval, G1K 7P4 Québec, QC, Canada (E-mail: *peter.vanrolleghem@gci.ulaval.ca*)

Abstract This contribution deals with the behaviour of a SHARON reactor for nitrogen removal from wastewater streams with high ammonium concentrations. A system analysis is performed on a two-step nitrification model, describing the behaviour of such a reactor. Steady states are identified through direct calculation using a canonical state space model representation. Practical operation of a SHARON reactor aims at reaching ammonium conversion to nitrite only (nitritation), while suppressing further conversion to nitrate. It is shown how this desired behaviour can be obtained by setting the dilution rate dependent on the influent ammonium concentration. The impact of microbial growth characteristics on the suitable operating region is examined, as well as the effect of reactor temperature and pH. Advice is given for robust reactor design and operation.

Keywords Nitrification; stability analysis; steady states; system analysis; wastewater treatment

Introduction

Biological processes for nitrogen removal from wastewater have proven their effectiveness and have been widely implemented. In the last few years, several novel nitrogen removal processes with improved sustainability have been developed. An example is the SHARON process (Single reactor system for High activity Ammonia Removal Over Nitrite), which is ideally suited to remove nitrogen from wastewater streams with high ammonium concentrations, such as the reject water originating from sludge digestion and dewatering (Hellinga *et al.*, 1998). In a SHARON reactor, typically a continuous stirred tank reactor (CSTR), ammonium is converted to nitrite (i.e. the nitritation reaction) while further conversion of nitrite to nitrate is prevented. At the prevailing pH (about 7) and high temperature (30–40 °C), ammonium oxidizers grow faster than nitrite oxidizers. By operating the reactor at a suitable dilution rate nitrite oxidizers are washed out while ammonium oxidizers stay in the reactor. In this way, substantial savings in aeration costs are realized, in comparison with complete oxidation of ammonium to nitrate.

Previous work has been devoted to the theoretical analysis of the SHARON reactor system. Using the contraction mapping theorem to identify regions in the input space for which a unique steady state exists, only the trivial wash-out state has been found - for very high values of the dilution rate (Volcke *et al.*, 2006), which is clearly not an interesting operating point. Volcke *et al.* (2007) have addressed the influence of microbial growth inhibition on steady state multiplicity and stability using a canonical state space model representation to calculate the steady state values. These studies have identified different steady state behaviours for different regions in the input space, i.e. the given influent ammonium concentration and the applied dilution rate. This contribution focuses

on the practical implications of these theoretical findings. It is examined how to optimize reactor operation and design to obtain the desired behaviour, i.e. ammonium oxidation to nitrite only. The study evaluates the influence of microbial kinetics (varying parameters or even structurally different growth kinetics) and operating conditions (temperature and pH) on practical reactor operation.

Methods

Two-step nitrification model under study

The simplified SHARON reactor model under study considers two nitrification reactions: oxidation of ammonium to nitrite and consecutive oxidation of nitrite to nitrate. The concentrations of the following four components are identified as the system's state variables: (total) ammonium $(S_{NH} = NH_4^+ + NH_3)$, (total) nitrite $(S_{NO2} = HNO_2 + NO_2^-)$, ammonium oxidizers (X_{AOB}) and nitrite oxidizers (X_{NOB}). These components are involved in two reactions: ammonium oxidation and nitrite oxidation, with respective biomass growth rates μ^{AOB} and μ^{NOB}. The reactor is modelled as a CSTR without biomass retention. The reactor liquid volume V is assumed constant, the flow rate is denoted by Q. The system's state equations are given by the individual mass balances:

$$
\begin{aligned}
\frac{dS_{NH}}{dt} &= \frac{Q}{V} \cdot \left(S_{NH}^{in} - S_{NH}\right) - \frac{1}{Y^{AOB}} \cdot \mu^{AOB}(\boldsymbol{x}) \cdot X_{AOB} - i_{NXB} \cdot \mu^{NOB}(\boldsymbol{x}) \cdot X_{NOB} \\
\frac{dS_{NO2}}{dt} &= -\frac{Q}{V} \cdot S_{NO2} + \left(\frac{1}{Y^{AOB}} - i_{NXB}\right) \cdot \mu^{AOB}(\boldsymbol{x}) \cdot X_{AOB} - \frac{1}{Y^{NOB}} \cdot \mu^{NOB}(\boldsymbol{x}) \cdot X_{NOB} \\
\frac{dX_{AOB}}{dt} &= -\frac{Q}{V} \cdot X_{AOB} + \mu^{AOB}(\boldsymbol{x}) \cdot X_{AOB} \\
\frac{dX_{NOB}}{dt} &= -\frac{Q}{V} \cdot X_{NOB} + \mu^{NOB}(\boldsymbol{x}) \cdot X_{NOB}
\end{aligned}
\tag{1}
$$

in which

$$
\begin{cases}
\mu^{AOB}(\boldsymbol{x}) = \mu_{max}^{AOB} \cdot \dfrac{S_{NH}}{K_{NH}^{AOB} + S_{NH}} \cdot \dfrac{K_{I,NO2}^{AOB}}{K_{I,NO2}^{AOB} + S_{NO2}} \\[2ex]
\mu^{NOB}(\boldsymbol{x}) = \begin{cases} \mu_{max}^{NOB} \cdot \dfrac{S_{NO2}}{K_{NO2}^{NOB} + S_{NO2}} & \text{for } S_{NH} > 0 \\[1ex] 0 & \text{for } S_{NH} = 0 \end{cases}
\end{cases}
\quad \text{and with } \boldsymbol{x} = \begin{bmatrix} x_1 \\ x_2 \\ x_3 \\ x_4 \end{bmatrix} = \begin{bmatrix} S_{NH} \\ S_{NO2} \\ X_{AOB} \\ X_{NOB} \end{bmatrix}
$$

The input variables are the dilution rate (Q/V) and the influent concentration of total ammonium (S_{NH}^{in}). The influent is assumed to contain neither nitrite nor biomass. The yield coefficients (Y^{AOB}, Y^{NOB}) and the nitrogen content of biomass (i_{NXB}) are constant stoichiometric coefficients. The maximum growth rates $(\mu_{max}^{AOB}, \mu_{max}^{NOB})$, substrate affinity constants $(K_{NH}^{AOB}, K_{NO2}^{NOB})$ and nitrite inhibition constant $(K_{I,NO2}^{AOB}$; model of Hellinga *et al.*, 1998) are kinetic parameters, which depend on temperature and pH (Table 1). For typical operating conditions (pH = 7 and T = 35 °C), the maximum growth rate of ammonium oxidizers is larger than the one of nitrite oxidizers $(\mu_{max}^{AOB} > \mu_{max}^{NOB})$. It is further assumed that the reactor is continuously aerated and oxygen is always present in excess, or at least a constant oxygen level is maintained (the influence of suboptimal oxygen levels is then comprised in μ_{max}^{AOB} and μ_{max}^{NOB}). Biomass decay has been neglected, a reasonable assumption when aiming at nitrite formation (working at not too low dilution rates).

Table 1 Default values of the SHARON model parameters (at pH $=7$ and T $=35\,°\text{C}$)

Symbol	Expression for T and pH dependency	Reference	Default value	Unit
μ_{max}^{AOB}	$2.22 \cdot 10^{11} \cdot \exp((-6.5 \cdot 10^4)/R \cdot T) \cdot (8.21/8.21 - 1 + 10^{\lvert 7.23 - pH \rvert})$	Hellinga *et al.* (1999) Van Hulle *et al.* (2007)	2.1	day^{-1}
K_{NH}^{AOB}	$5.357 \cdot 10^{-2} \cdot (1 + (10^{-pH}/K_{e,NH_4^+})); K_{e,NH_4^+} = \exp(-6344/T)$	Van Hulle *et al.* (2007) Anthonisen *et al.* (1976)	4.73	mole m^{-3}
$K_{I,NO2}^{AOB}$	$0.146 \cdot (1 + (K_{e,HNO_2}/10^{-pH})); K_{e,HNO_2} = \exp(-2300/T)$	Van Hulle *et al.* (2007) Anthonisen *et al.* (1976)	837	mole m^{-3}
μ_{max}^{NOB}	$4.50 \cdot 10^7 \cdot \exp(-4.5 \cdot 10^4/R \cdot T) \cdot (8.21/(8.21 - 1 + 10^{\lvert 7.23 - pH \rvert}))$	Hellinga *et al.* (1999) Van Hulle *et al.* (2007)	1.05	day^{-1}
K_{NO2}^{NOB}	$6.8 \cdot 10^{-5} \cdot (1 + (K_{e,HNO_2}/10^{-pH})); K_{e,HNO_2} = \exp(-2300/T)$	Wiesmann (1994) Anthonisen *et al.* (1976)	0.39	mole m^{-3}
Y_{AOB}	–	Hellinga *et al.* (1999)	0.0625	mole mole^{-1}
i_{NXB}	–	Typical textbook value	0.2	mole mole^{-1}
Y_{NOB}	–	Hellinga *et al.* (1999)	0.017	mole mole^{-1}

Canonical state space model representation

By defining new state space variables **y**:

$$
\mathbf{y} = \begin{bmatrix} y_1 \\ y_2 \\ y_3 \\ y_4 \end{bmatrix} \equiv \begin{bmatrix} S_{\mathrm{NH}} + 1/Y^{\mathrm{AOB}} \cdot X_{\mathrm{AOB}} + i_{\mathrm{NXB}} \cdot X_{\mathrm{NOB}} \\ S_{\mathrm{NO2}} - \left(1/Y^{\mathrm{AOB}} - i_{\mathrm{NXB}}\right) \cdot X_{\mathrm{AOB}} + 1/Y^{\mathrm{NOB}} \cdot X_{\mathrm{NOB}} \\ X_{\mathrm{AOB}} \\ X_{\mathrm{NOB}} \end{bmatrix}
$$

$$
\Rightarrow \quad \begin{aligned} \dot{y}_1 &= Q/V \cdot \left(S_{\mathrm{NH}}^{\mathrm{in}} - y_1\right) \\ \dot{y}_2 &= -Q/V \cdot y_2 \\ \dot{y}_3 &= \left(-Q/V + \lambda^{\mathrm{AOB}}(\mathbf{y})\right) \cdot y_3 \\ \dot{y}_4 &= \left(-Q/V + \lambda^{\mathrm{NOB}}(\mathbf{y})\right) \cdot y_4 \end{aligned} \tag{2}
$$

with $\lambda^i(\mathbf{y}) = \mu^i(\mathbf{x}); i = $ AOB,NOB, the model is brought in a canonical form (Bastin and Dochain, 1990), which consists of a linear part of dimension 2 coupled with a nonlinear part of dimension 2. The state variables x_i (i = 1,…4) of the two-step nitrification model (Equation 1) cannot become negative. Call S_y the image of $\Re^{+,4} \equiv \left\{x \in \Re^4 : x_i \geq 0, \ i = 1,…4\right\}$ under the transformation $\mathbf{x} \mapsto \mathbf{y}$. S_y is the state space of the system defined by Equations 2. Every trajectory that starts at $t = 0$ in a point $\mathbf{y_0}$ of S_y, stays in S_y for $t \geqq 0$. It subsequently converges (for positive constant input values Q/V and $S_{\mathrm{NH}}^{\mathrm{in}}$) to the cross-section Δ of S_y with the plane $\left\{y_1 = S_{\mathrm{NH}}^{\mathrm{in}}, \ y_2 = 0\right\}$. Δ is a bounded region, defined by

$$
S_{\mathrm{NH}}^{\mathrm{in}} - 1/Y^{\mathrm{AOB}} \cdot y_3 - i_{\mathrm{NXB}} \cdot y_4 \geq 0; \ (1/Y^{\mathrm{AOB}} - i_{\mathrm{NXB}}) \cdot y_3 - 1/Y^{\mathrm{NOB}} \cdot y_4 \geq 0; \ y_3 \geq 0; \ y_4 \geq 0 \tag{3}
$$

The process converges to a second order behaviour that is determined by the dynamics of y_3 ($= X_{\mathrm{AOB}}$) and y_4 ($= X_{\mathrm{NOB}}$).

Results and discussion

Steady state behaviour

Using the canonical state space model representation, the direct calculation of steady states of the model is substantially simplified. For positive dilution rates and influent ammonium concentrations ($Q/V > 0$ and $S_{\mathrm{NH}}^{\mathrm{in}} > 0$), up to three physical steady states are obtained. Figure 1 depicts the regions in the input space ($Q/V, S_{\mathrm{NH}}^{\mathrm{in}}$) for which the number and the stability of the steady states differ. The equations of the boundaries between the different operating regions are also included. The stability of the steady states in the different regions in the input space has been assessed using the linearization principle (Table 2). Three different regions in the input space are distinguished.

- For high dilution rates Q/V or low influent ammonium concentrations $S_{\mathrm{NH}}^{\mathrm{in}}$ (zone A), only the wash-out state $\bar{\mathbf{x}}^{\mathbf{A}}$ is a physical steady state.
- For moderately high dilution rates Q/V and somewhat high influent ammonium concentrations $S_{\mathrm{NH}}^{\mathrm{in}}$ (zone AB), the system possesses two physical steady states. The wash-out state $\bar{\mathbf{x}}^{\mathbf{A}}$ is now unstable. The second steady state, $\bar{\mathbf{x}}^{\mathbf{B}}$, corresponds with only nitrite formation. This steady state is *quasi* globally asymptotically stable, in the sense that all trajectories within the physical boundaries of the system converge to this point, *except* the trivial trajectory coinciding with $\bar{\mathbf{x}}^{\mathbf{A}}$, the latter corresponding with a situation in which initially no biomass is present in the reactor.
- For sufficiently low dilution rates Q/V and corresponding influent ammonium concentrations $S_{\mathrm{NH}}^{\mathrm{in}}$ (zone ABC), three steady states occur. The wash-out state $\bar{\mathbf{x}}^{\mathbf{A}}$ is still unstable. The second steady state, $\bar{\mathbf{x}}^{\mathbf{B}}$, corresponding with only nitrite formation, is
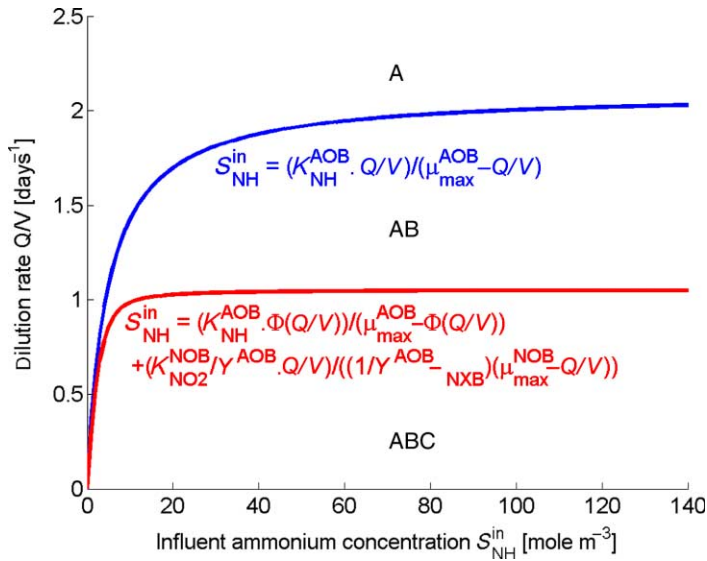
Figure 1 Occurrence of steady states in terms of the input variables S_{NH}^{in} and Q/V ($*$) ($*$) with $\phi(Q/V) = (Q/V) + (K_{NO2}^{NOB} \cdot (Q/V)^2 / K_{I,NO2}^{AOB} \cdot (\mu_{max}^{NOB} - Q/V))$

now also unstable: only trajectories on the x_3-axis converge to $\bar{\mathbf{x}}^B$, corresponding with a reactor with initially only ammonium oxidizers present (no nitrite oxidizers are supposed to enter the reactor so nitrite oxidation cannot even start). The third steady state, $\bar{\mathbf{x}}^C$, corresponding with nitrate formation, is *quasi* globally asymptotically stable: all trajectories within the physical boundaries of the system converge to this point, *except for* the steady state $\bar{\mathbf{x}}^A$ and the trajectories on the x_3-axis.

In each input region, the (quasi) g.a.s. steady state will be reached, independent of the initial conditions (apart from given exceptions). Figure 2 displays the corresponding phase trajectories in the cross-section Δ of S_y with the plane $\{y_1 = S_{NH}^{in},\ y_2 = 0\}$. More details can be found in Volcke (2006).

Practical implications: setting the appropriate dilution rate

Good operation of a SHARON reactor aims at ammonium oxidation to nitrite only. Qualitatively, this is achieved by applying a dilution rate that is high enough to wash-out nitrite oxidizers, but low enough to ensure growth of ammonium oxidizers. This rule of thumb has been confirmed by the results in the previous section, where zone AB corresponds with the desired operating region. However, from Figure 1, it is clear that the influent ammonium concentration also plays a role in finding an appropriate dilution rate: for decreasing influent ammonium concentrations, the dilution rate should be kept lower to

Table 2 Stability of steady states

Operating region	Physical steady state	Stability
A	$\bar{\mathbf{x}}^A$	g.a.s.
AB	$\bar{\mathbf{x}}^A$	unstable
	$\bar{\mathbf{x}}^B$	*quasi* g.a.s.
ABC	$\bar{\mathbf{x}}^A$	Unstable
	$\bar{\mathbf{x}}^B$	Unstable
	$\bar{\mathbf{x}}^C$	*quasi* g.a.s.

*g.a.s. = globally asymptotically stable *quasi*: except for the trajectories mentioned in the text
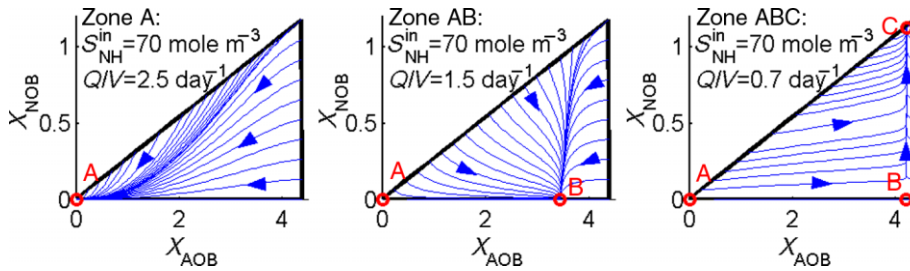
Figure 2 Trajectory fields for the different regions in the input space (Q/V, S_{NH}^{in})

prevent biomass wash-out. This reveals the need to appropriately design the reactor volume not only for a given reject water flow rate but also for its ammonium concentration. If the range of influent ammonium concentrations to be treated is known in advance, e.g.$50–85$ mole m^{-3} or about $700–1200$ gNm^{-3}, one can determine the range of dilution rates that guarantee stable nitrite formation, in this case $0.96–1.77$ day^{-1}, so $Q/V = 1.4$ day^{-1} would be a good choice to ensure robust operation (Figure 3 – left). For a given reactor volume V, this information can be used to control the influent flow rate Q, at least between certain ranges (this will probably require a buffer tank in front of the SHARON reactor). As an alternative, one could opt for a variable volume. This information can also be used during the design phase, to determine the reactor volume V that guarantees stable nitrite formation for an expected range of influent ammonium concentrations and influent flow rates. However, Figure1 reveals that the boundaries, which separate the operating regions A, AB and ABC with $\bar{x}^A$, $\bar{x}^B$, or $\bar{x}^C$ respectively as the (quasi) globally asymptotically stable steady state, depend on the microbial characteristics (μ_{max}^{AOB}, μ_{max}^{NOB}, K_{NH}^{AOB}, K_{NO2}^{NOB}, $K_{I,NO2}^{AOB}$, Y^{AOB} and i_{NXB}), which can only be estimated at the design stage. This demonstrates again the usefulness of aiming at maximum robustness.

Influence of parameter values characterizing microbial growth

Microbial characteristics clearly have an impact on the operating conditions for which stable nitrite formation is obtained. It is known from practice that the operating region in which stable nitrite formation is obtained, becomes larger when the difference between the maximum growth rates of ammonium oxidizers (μ_{max}^{AOB}) and nitrite oxidizers (μ_{max}^{NOB}) becomes larger, e.g. when the temperature increases. Besides, it is clear from this study that also the values of the substrate affinity constants (K_{NH}^{AOB} and K_{NO2}^{NOB}) and inhibition constants ($K_{I,NO2}^{AOB}$) play a role, as well as the value of the yield coefficient of ammonium oxidizers (Y^{AOB}) and even the nitrogen content of biomass (i_{NXB}). It is expected that slight deviations of parameter values that have been estimated initially (e.g. due to changing biomass characteristics with time) will not significantly affect the steady state
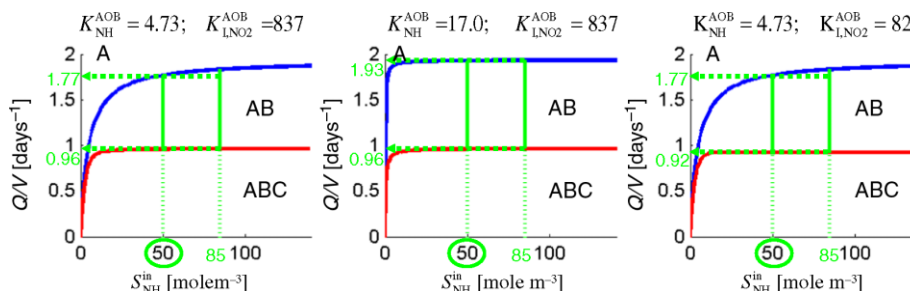
Figure 3 Practical use of the diagrams in establishing only nitrite formation. Left: default parameter values; middle: influence of K_{NH}^{AOB}; right: influence of $K_{I,NO2}^{AOB}$

behaviour, at least if one ensures not to operate too close to the boundaries that separate the different regions A, AB and ABC. Nevertheless, it is interesting to study the effect of the ammonium affinity constant and nitrite inhibition constant of ammonium oxidizers, for which quite varying values can be found in literature. Besides, drastic parameter changes can be caused by changing operating conditions in terms of temperature and pH of which the effect is worth examining more closely.

Influence of the ammonium affinity constant of ammonium oxidizers, K_{NH}^{AOB}. This parameter determines the steepness of the A/AB boundary: it corresponds to the influent ammonium concentration S_{NH}^{in} for which this boundary reaches half of its maximum value (in terms of Q/V). A decreasing K_{NH}^{AOB}-value also corresponds to a steeper AB/ABC boundary, although this effect is less pronounced (the value of K_{NO2}^{NOB} plays a similar role here). With respect to reactor operation, an increasing ammonium affinity (lower K_{NH}^{AOB}-value) reduces the influence of the influent ammonium concentration on the range of dilution rates for which only nitrite formation is established. This is illustrated considering $K_{NH}^{AOB} = 0.17\,\text{mole m}^{-3}$ (Wiesmann, 1994), a typical value although rather low for nitrifiers in the SHARON process, which puts a selection pressure on fast growth rate rather than substrate affinity. When treating influent ammonium concentrations of $50-85\,\text{mole m}^{-3}$, stable nitrite formation is realized for a larger range of dilution rates ($0.96-1.93\,\text{day}^{-1}$, Figure 3 – middle).

Influence of the nitrite inhibition constant of ammonium oxidizers $K_{I,NO2}^{AOB}$. As ammonium oxidation becomes more severely inhibited by nitrite (decreasing $K_{I,NO2}^{AOB}$), the AB/ABC boundary shifts more and more down, so the region AB becomes larger. This can be explained by the fact that the nitrite concentration corresponding with the steady state with only nitrite formation ($\bar{\mathbf{x}}^{\mathbf{B}}$) becomes lower as nitrite inhibition increases (Volcke, 2006). In other words, nitrite inhibition of ammonium oxidation leads to substrate limitation of the subsequent nitrite oxidation step. Figure 3 (right) displays the results for $K_{I,NO2}^{AOB} = 82\,\text{mole m}^{-3}$ (Hellinga *et al.*, 1998), although the effect is not very pronounced: for $S_{NH}^{in} = 50-85\,\text{mole m}^{-3}$, nitrite formation is now established for $Q/V = 0.92 - 1.77\,\text{day}^{-1}$.

Influence of reactor temperature. The reactor temperature directly affects the maximum growth rates of ammonium oxidizers (μ_{max}^{AOB}) and nitrite oxidizers (μ_{max}^{NOB}): as the temperature increases, both values increase, as does the relative difference between them. The affinity and inhibition constants are indirectly affected by the reactor temperature (through the equilibrium coefficients, Table 1), but this effect is only minor in the normal operating temperature range of a SHARON reactor ($30-40\,^{\circ}\text{C}$). Overall, the operating region AB in which only nitrite formation is obtained, becomes larger as temperature increases (Figure 4). At low temperatures the region AB becomes so small that obtaining only nitrite formation is practically impossible without risking complete biomass wash-out.

Influence of reactor pH. The maximum growth rates μ_{max}^{AOB} and μ_{max}^{NOB} are the largest at the optimum pH-value of 7.23 (assumed to be the same for both species), while their values decrease at lower as well as higher pH-values. This is reflected in the position of the A/AB and AB/ABC boundaries, which are the highest near the optimum pH-value of 7.23. Besides, at increasing pH values, the ammonium affinity constant K_{NH}^{AOB} decreases, while the nitrite affinity constant K_{NO2}^{NOB} and the nitrite inhibition constant $K_{I,NO2}^{AOB}$ increase, reflecting the relative increase of uncharged ammonia (NH_3) and the relative decrease of uncharged nitrous acid (HNO_2), being the actual substrates or inhibiting component. As
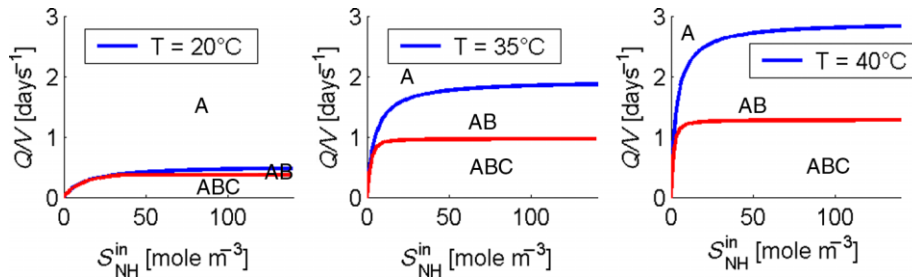
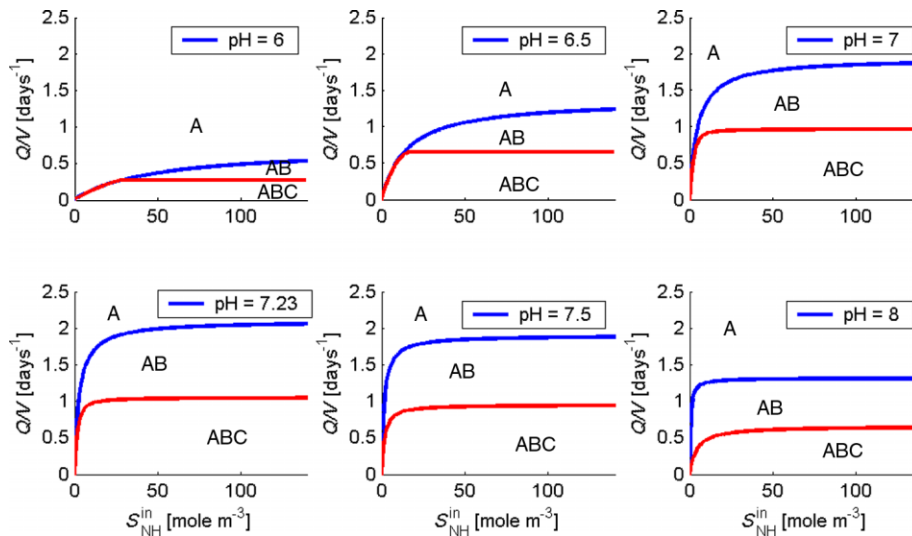**Figure 4** Influence of reactor temperature on the occurrence of steady states (at pH $=$ 7) in terms of the influent ammonium concentration S_{NH}^{in} [mole m^{-3}] and the dilution rate Q/V [days^{-1}]

K_{NH}^{AOB} decreases for increasing pH, the boundary between the A and AB regions reaches its maximum value (μ_{max}^{AOB}) for lower S_{NH}^{in}−values: the influence of the influent ammonium concentration on the optimal dilution rate for obtaining only nitrite formation, becomes less pronounced with respect to the transition between the wash-out state and the steady state with only nitrite formation. The boundary between the AB and ABC regions displays an opposite trend, reaching its maximum value only at higher S_{NH}^{in}−values for increasing pH (7 → 8) because of the associated increase of K_{NO2}^{NOB}. At low pH values (6−6.5), the latter effect is however dominated by decreasing K_{NH}^{AOB}, also influencing the position of the AB/ABC boundary, which is always below the A/AB boundary. The decreasing nitrite inhibition effect (increasing $K_{I,NO2}^{AOB}$) with increasing pH causes the AB/ABC boundary to shift upwards, although this effect is hardly noticeable for the low nitrite inhibition level considered in this study. Overall (Figure 5), as for reactor operation, the input region corresponding with only nitrite formation is the largest around the pH-value corresponding with the highest maximum growth rates (pH $\geq$ 7.23).

Influence of microbial growth kinetics - inhibition effects

Besides the microbial growth parameters, also the structure of the microbial growth rates μ^{AOB} and μ^{AOB}, more specifically the inhibition kinetics, will affect the operating

Figure 5 Influence of reactor pH on the occurrence of steady states (at $T = 35\,^{\circ}$C) in terms of the influent ammonium concentration S_{NH}^{in} [mole m^{-3}] and the dilution rate Q/V [days^{-1}]
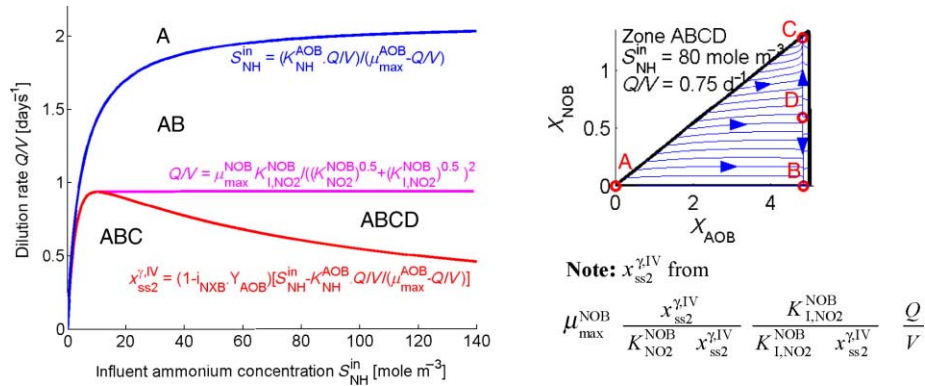
Figure 6 Occurrence of steady states in terms of the input variables in case of nitrite inhibition of nitrite oxidation (left); trajectory fields in zone ABCD (right)

conditions for which stable nitrite formation is achieved, particularly in case of substrate inhibition (Volcke *et al.*, 2007).

Figure 6 shows the results in case of nitrite inhibition of nitrite oxidation (Haldane kinetics), with inhibition constant $106 \, \text{mole m}^{-3}$ (Wiesmann, 1994), resulting in the occurrence of up to 4 steady states. In the operating zone AB, nitrite formation only is always achieved. However, also working in the region ABCD can now also lead to nitrite formation only. In this case, both the steady state with only nitrite formation (B) and a steady state with nitrate formation (C), are locally asymptotically stable. The initial conditions will now determine which of these stable steady states is reached. The stability boundary, that separates their attraction regions is formed by the trajectories that are attracted to the steady state D, also corresponding with nitrate formation, which is unstable. Overall, the operating region in which only nitrite is formed, becomes larger. Note that its boundaries show again a clear influence of the influent ammonium concentration.

Conclusions

This contribution assesses the influence of operating conditions and microbial kinetics on the practical operation of a SHARON partial nitritation reactor. Whether the desired behaviour - ammonium oxidation to nitrite only - is obtained, does not only depend on the dilution rate, as is commonly known, but is also influenced by the influent ammonium concentration. The latter is attributed to the low substrate affinity of nitrifiers in a SHARON reactor, as well as to the different inhibition levels and types to which they may be subjected.

Microbial growth characteristics clearly have an impact on the operating conditions for which stable nitrite formation is obtained. While changing growth parameter values, e.g. because of changing reactor temperature or pH, only have quantitative effects, the type of microbial (inhibition) kinetics may even qualitatively affect the results, i.e. the number of steady states and their stability. Advice is given for robust reactor design, aiming at working in the middle of the operating zone for which only nitrite formation is achieved.

References

Anthonisen, A.C., Loehr, R.C., Prakasam, T.B.S. and Srinath, E.G. (1976). Inhibition of nitrification by ammonia and nitrous acid. *Journal WPCF*, **48**, 835–852.

Bastin, G. and Dochain, D. (1990). *On-line Estimation and Adaptive Control of Bioreactors*, Elsevier, Amsterdam, pp. 29–46.

Hellinga, C., Schellen, A.A.J.C., Mulder, J.W., van Loosdrecht, M.C.M. and Heijnen, J.J. (1998). The SHARON process: an innovative method for nitrogen removal from ammonium-rich wastewater. *Wat. Sci. Tech.*, **37**(9), 135–142.

Hellinga, C., van Loosdrecht, M.C.M. and Heijnen, J.J. (1999). Model based design of a novel process for nitrogen removal from concentrated flows. *Math. Comp. Modell. Dyn. Sys.*, **5**, 351–371.

Van Hulle, S.W.H., Volcke, E.I.P., Teruel, J.L., Donckels, B., van Loosdrecht, M.C.M. and Vanrolleghem, P.A. (2007). Influence of temperature and pH on the kinetics of the SHARON nitritation process. *J. Chem. Technol. Biot.*, **82**(5), 471–480.

Volcke E.I.P. (2006). *Modelling, analysis and control of partial nitration in a SHARON reactor*. PhD thesis, Ghent University, Belgium, 300p. Available on http://biomath.ugent.be/publications/download/VolckeEveline_PhD.pdf.

Volcke, E.I.P., Loccufier, M., Vanrolleghem, P.A. and Noldus, E.J.L. (2006). Existence, uniqueness and stability of the equilibrium points of a SHARON bioreactor model. *J. Process. Contr.*, **16**, 1003–1012.

Volcke, E.I.P., Sbarciog, M., Loccufier, M., Vanrolleghem, P.A. and Noldus, E.J.L. (2007). Influence of microbial growth kinetics on steady state multiplicity and stability of a two-step nitrification (SHARON) model. *Biotechnol. Bioeng*. in press (DOI: 10.1002/bit.21464).

Wiesmann, U. (1994). Biological nitrogen removal from wastewater. In: *Advances in Biochemical Engineering/Biotechnology*, (**51**)., Fiechter, A. (ed.), Springer-Verlag, Berlin, pp. 113–154.

E.I.P. Volcke et al.